A Robust and Efficient Algorithm for Coprime Array Adaptive Beamforming

Chengwei Zhou, *Student Member, IEEE*, Yujie Gu, *Senior Member, IEEE*, Shibo He, *Member, IEEE*, and Zhiguo Shi, *Senior Member, IEEE*

***Abstract*—Coprime array offers a larger array aperture than uniform linear array with the same number of physical sensors, and has a better spatial resolution with increased degrees of freedom. However, when it comes to the problem of adaptive beamforming, the existing adaptive beamforming algorithms designed for the general array cannot take full advantage of coprime feature offered by the coprime array. In this paper, we propose a novel coprime array adaptive beamforming algorithm, where both robustness and efficiency are well balanced. Specifically, we first decompose the coprime array into a pair of sparse uniform linear subarrays and process their received signals separately. According to the property of coprime integers, the direction-of-arrival (DOA) can be uniquely estimated for each source by matching the super-resolution spatial spectra of the pair of sparse uniform linear subarrays. Further, a joint covariance matrix optimization problem is formulated to estimate the power of each source. The estimated DOAs and their corresponding power are utilized to reconstruct the interference-plus-noise covariance matrix and estimate the signal steering vector. Theoretical analyses are presented in terms of robustness and efficiency, and simulation results demonstrate the effectiveness of the proposed coprime array adaptive beamforming algorithm.**

***Index Terms*—Adaptive beamforming, coprime array, DOA estimation, joint covariance matrix optimization, reconstruction.**

I. Introduction

ADAPTIVE beamforming is one of the fundamental signal processing techniques, and has been widely applied in mobile wireless communications to receive the desired user signal while suppress the interference and noise by dynamically adjusting the beamformer weights of the array [1]–[5]. It is quite common in, for example, cellular network, mobile relay system and secure communication, that non-ideal propagation environments or conditions can be encountered due to channel uncertainty, signal pointing error, local scattering effect, and wavefront distortions [6]–[8]. Moreover, a limited number of samples caused by the fast time-varying statistics is also a typical characteristic in practical mobility applications. In order to meet the increasing user demands and guarantee the overall system performance, both better robustness and higher efficiency are desirable for adaptive beamformers.

There has been a long line of adaptive beamforming algorithms, where uniform linear array (ULA) is the most commonly adopted array configuration since it satisfies the Nyquist sampling theorem [3], [9]. It is worth noting that a trade-off should be made between the performance requirements and the computational complexity. More specifically, a larger array aperture means higher resolution and stronger interference rejection capability. For a ULA, enlarging the array aperture via adding sensors implies increased hardware and computational complexity. As such, exploiting non-uniform sparse array becomes a preferred choice to achieve a larger array aperture without increasing the number of sensors.

Coprime array is a newly emerged non-uniform sparse array, which has a larger array aperture than the ULA with the same number of sensors [10]. It has been shown that coprime array has provable performance guarantees with less sensors. By exploiting the property of coprime array, researches have been carried out on high resolution direction-of-arrival (DOA) estimation with increased degrees of freedom (DOFs), where the estimation is accomplished by processing the equivalent received signal of the virtual array with more virtual sensors [10]–[15]. In contrast, there are few results on adaptive beamforming for the coprime array. In [16], a coprime array adaptive beamforming algorithm was proposed by establishing a connection between the coprime array and its derived virtual ULA; hence, existing adaptive beamforming algorithms designed for ULA can be adopted. By processing the equivalent virtual ULA received signal, a significant output performance increment can be achieved. However, model mismatch still exists since the sample covariance matrix generated from the virtual array is contaminated by the desired signal component.

To mitigate the performance degradation caused by model mismatch, the idea of recently proposed covariance matrix reconstruction [17]–[19] can be borrowed, which provides a signal-free interference-plus-noise covariance matrix. Based on the minimum variance distortionless response (MVDR)

Manuscript received January 16, 2017; revised March 19, 2017; accepted April 23, 2017. Date of publication May 16, 2017; date of current version February 12, 2018. This work was supported in part by Zhejiang Provincial Natural Science Foundation of China under Grant LR16F010002, in part by the National Natural Science Foundation of China under Grant U1401253, and in part by the Fundamental Research Funds for the Central Universities under Grant 2017QNA5009. This paper was presented in part at the IEEE International Conference on Acoustics, Speech and Signal Processing, Shanghai, China, March 2016. The review of this paper was coordinated by Prof. C. Yuen. *(Corresponding author: Zhiguo Shi.)*

C. Zhou and Z. Shi are with the College of Information Science and Electronic Engineering, Zhejiang University, Hangzhou 310027, China (e-mail: zhouchw@zju.edu.cn; shizg@zju.edu.cn).

Y. Gu is with the Department of Electrical and Computer Engineering, Temple University, Philadelphia, PA 19122 USA (e-mail: guyujie@hotmail.com).

S. He is with the State Key Laboratory of Industrial Control Technology, College of Control Science and Engineering, Zhejiang University, Hangzhou 310027, China (e-mail: s18he@iipc.zju.edu.cn).

Color versions of one or more of the figures in this paper are available online at http://ieeexplore.ieee.org.

Digital Object Identifier 10.1109/TVT.2017.2704610

principle, the beamformer weight is a function of the interference-plus-noise covariance matrix and the desired signal steering vector. Recalling their definitions, the DOA and power of each source are the key parameters for reconstructing the interference-plus-noise covariance matrix and estimating the desired signal steering vector. Hence, the accuracy of DOA and power estimation will directly affect the output performance of a reconstruction-based adaptive beamformer.

Considering the fact that the resolution is proportional to the array aperture, coprime array is a good candidate to achieve a higher resolution with less sensors because of its sparse sensor deployment. Nevertheless, its non-uniformity limits the incorporation of existing adaptive beamforming algorithms mainly designed for ULAs. In order to take advantages of the coprime feature, we propose a novel robust and efficient coprime array adaptive beamforming algorithm in this paper, where the DOA and power for adaptive beamformer design are estimated based on the decomposed coprime sub-arrays. Specifically, we propose a spatial spectra matching scheme to estimate the DOAs of the desired signal and interferers, where two spatial spectra corresponding to the pair of decomposed sparse uniform linear sub-arrays are matched for unique estimation. To eliminate the phase ambiguity caused by the sparse sensor deployment, the existence and uniqueness of DOA estimation are proved according to the property of coprime integers. Subsequently, with the estimated DOAs, a joint covariance matrix optimization problem is formulated to estimate the sources power. The estimated DOAs and power are used to reconstruct the interference-plus-noise covariance matrix and estimate the desired signal steering vector, based on which the MVDR beamformer can be calculated. Theoretical analyses are provided to verify the robustness and efficiency of coprime array adaptive beamforming. Extensive simulation results demonstrate that the proposed algorithm is robust to typical model mismatches in practical mobile wireless communication applications, and can obtain near-optimal output performance in a high dynamic range.

The main contribution of this paper is threefold:

1) We design a robust and efficient adaptive beamforming algorithm tailored for the coprime array, whose coprime feature can be incorporated to improve the output performance with a reasonable computational complexity;
2) We analyze the key parameters affecting the performance of MVDR beamformer, and propose to perform DOA and power estimation based on the pair of decomposed coprime sub-arrays for adaptive beamformer design;
3) We investigate the spatial spectrum characteristic of the pair of decomposed sparse uniform linear sub-arrays, and verify the feasibility of DOA estimation from the perspective of existence and uniqueness.

The rest of this paper is organized as follows. In Section II, we present the review of related work. In Section III, we describe the preliminaries of this paper, including coprime array signal model and the motivation of this work. In Section IV, we elaborate the proposed coprime array adaptive beamforming algorithm, and theoretical analyses are provided in Section V. Simulation results are presented in Section VI for comparison. Finally, we conclude this paper in Section VII.

II. Related Work

A. Coprime Array Signal Processing

The concept of coprime sampling was first proposed by Vaidyanathan and Pal in [10], where a pair of coprime sparse samplers was utilized to undersample the signals. As one of typical implementations of coprime sampling, coprime array provides a systematical framework for sparse array configuration, and has found broad applications in radar, sonar, acoustics, seismology, medical imaging, and wireless communications [20]–[24]. Compared to the ULA with the same number of physical sensors, the sparse non-uniform coprime array has a larger array aperture. Moreover, with a coprime pair of sparse uniform linear sub-arrays, both the coprime feature and the sparse ULA properties can be utilized to promote the signal processing performance.

Most of the existing literatures on coprime array signal processing are focused on DOA estimation, where two pursuits are included, namely, high resolution and increased DOFs. To achieve a high resolution, the large array aperture of coprime array was utilized in [25], [26], where both resolution and computational efficiency were significantly improved. To obtain an increased DOFs, a much longer virtual array was derived by calculating the difference coarray of coprime array in [10], where there are more virtual sensors than physical sensors. By conducting the equivalent virtual array signal, the available DOFs can be significantly increased through spatial smoothing [15], [27], sparse reconstruction [11], [13], compressive sensing [14], etc. In addition, the Toeplitz characteristic of covariance matrix was also investigated in [28]–[30] to perform efficient spectrum estimation. However, to the best of our knowledge, there is little work on adaptive beamforming for the coprime array.

It is worth noting that the intention of adaptive beamforming is different from the DOA estimation algorithms reviewed above. In detail, DOA estimation can be accomplished by utilizing the equivalent virtual difference coarray signal derived from the coprime array, which belongs to the second-order statistics containing the power of each source. In contrast, the output of an adaptive beamformer is a weighted signal waveform instead of a weighted signal power; hence, the adaptive beamformer should be weighted to the physical sensors in the coprime array rather than to the virtual sensors in the derived virtual array. Therefore, the solutions based on the derived virtual array for DOA estimation cannot be directly applied to coprime array adaptive beamforming.

B. Reconstruction-Based Beamformer Design Principle

Among the various adaptive beamformers, the recently proposed interference-plus-noise covariance matrix reconstruction-based beamformer has attracted extensive concern due to its distinctive design principle and superior overall performance. In [17], Gu and Leshem reconstructed the interference-plus-noise covariance matrix by integrating the Capon spatial spectrum over the interference angular region, so that the desired signal component can be effectively excluded from the reconstructed covariance matrix. However, its computational complexity is

high since all angles within the potential interference angular region are involved in the reconstruction process. Moreover, the underestimated interferences power via Capon spatial spectrum also has an impact on the accuracy of the reconstructed covariance matrix. In [18], the integral operation for interference-plus-noise covariance matrix reconstruction was simplified to a summation operation through exploiting the sparsity of incident sources over the spatial domain.

Note that the reconstruction-based beamforming algorithms mentioned above are designed for the general array configuration, among which ULA is the most popular one. With a ULA, enlarging the array aperture is at the cost of increasing the system complexity. More importantly, the existing adaptive beamforming algorithms designed for the general array cannot take full advantage of coprime feature offered by the coprime array, and may suffer performance degradation caused by the non-uniform sparse sensor deployment. Consequently, it is necessary to develop a more efficient and effective adaptive beamforming approach tailored for the coprime array.

III. Preliminaries

In this section, we first describe the coprime array signal model for adaptive beamforming, then present the motivation of this work.

Throughout this paper, vectors and matrices are denoted by lower case and upper case boldface characters, respectively. The superscripts $(\cdot)^T$ and $(\cdot)^H$ respectively denote the transpose and conjugate transpose operation, and $(\cdot)^\star$ denotes the optimal solution to the optimization problem. The notation $E[\cdot]$ denotes the statistical expectation operator, and $\|\cdot\|_F$ denotes the Frobenius norm. $\mathrm{diag}(\cdot)$ represents a diagonal matrix with the corresponding elements on its diagonal, and $\mathrm{vec}(\cdot)$ stands for the vectorization operator. $\mathbf{0}$ denotes the zero matrix of appropriate dimension. Finally, $\mathbf{I}$ denotes the identity matrix with appropriate dimension unless otherwise specified.

A. Coprime Array Signal Model

Denote M and N as a pair of coprime integers. Coprime array is the union of two sparse uniform linear sub-arrays consisting of M and N sensors, respectively. As shown in Fig. 1(a), the sub-array with M sensors has an inter-element spacing of Nd, whereas the sub-array with N sensors has an inter-element spacing of Md. Here, the unit spacing d is chosen to be a half-wavelength without loss of generality. With the first sensor of each sub-array serving as the common reference, the coprime array configuration shown in Fig. 1(b) consists of $M+N-1$ sensors with an array aperture of $\max((M-1)Nd, (N-1)Md)$.

Assume that there are $K+1$ far-field narrowband signals impinging on the coprime array. Among them, the signal from θ_s is regarded as the desired signal and the others from $\{\theta_k, k=1,2,\ldots,K\}$ are interferers. The $(M+N-1)$-dimensional complex-valued received signal vector at the l-th snapshot can be modeled as

$$\mathbf{x}(l) = \mathbf{s}(l) + \mathbf{i}(l) + \mathbf{n}(l), \tag{1}$$

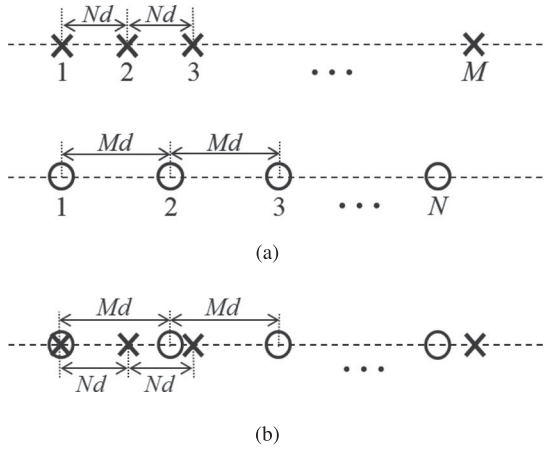

Fig. 1. Coprime array configuration. (a) Decomposed: A pair of sparse uniform linear sub-arrays; (b) aligned: A non-uniform linear array.

where $\mathbf{s}(l) = \mathbf{d}(\theta_s)s(l)$, $\mathbf{i}(l)$ and $\mathbf{n}(l)$ denote the statistically independent desired signal component, interference component and Gaussian noise component, respectively. Here, $\mathbf{d}(\theta_s)$ denotes the steering vector of the desired signal waveform $s(l)$.

The adaptive beamformer output is given by

$$y(l) = \mathbf{w}^H\mathbf{x}(l), \tag{2}$$

where $\mathbf{w} \in \mathbb{C}^{M+N-1}$ denotes the beamformer weight vector. The array output signal-to-interference-plus-noise ratio (SINR), defined as

$$\mathrm{SINR} = \frac{\sigma_s^2\left|\mathbf{w}^H\mathbf{d}(\theta_s)\right|^2}{\mathbf{w}^H\mathbf{R}_{i+n}\mathbf{w}}, \tag{3}$$

can be utilized to measure the beamformer performance, where $\sigma_s^2 = E[|s(l)|^2]$ denotes the desired signal power, and

$$\begin{aligned}\mathbf{R}_{i+n} &= E\left[\big(\mathbf{i}(l)+\mathbf{n}(l)\big)\big(\mathbf{i}(l)+\mathbf{n}(l)\big)^H\right] \\ &= \sum_{k=1}^{K}\sigma_k^2\mathbf{d}(\theta_k)\mathbf{d}^H(\theta_k) + \sigma_n^2\mathbf{I}\end{aligned} \tag{4}$$

denotes the interference-plus-noise covariance matrix. Here, σ_k^2 and σ_n^2 denote the power of the k-th interference and noise, respectively. Maximizing the array output SINR (3) is equivalent to minimize the array output variance while maintain the desired signal undistorted as

$$\min_{\mathbf{w}} \ \mathbf{w}^H\mathbf{R}_{i+n}\mathbf{w} \quad \text{subject to} \quad \mathbf{w}^H\mathbf{d}(\theta_s) = 1, \tag{5}$$

whose solution

$$\mathbf{w} = \frac{\mathbf{R}_{i+n}^{-1}\mathbf{d}(\theta_s)}{\mathbf{d}^H(\theta_s)\mathbf{R}_{i+n}^{-1}\mathbf{d}(\theta_s)} \tag{6}$$

is known as the MVDR beamformer [31].

Considering the fact that $\mathbf{R}_{i+n}$ is unavailable in practice since we cannot only pick up the interference and noise components from the received signal $\mathbf{x}(l)$, it is usually replaced by the sample

covariance matrix

$$\hat{\mathbf{R}} = \frac{1}{L}\sum_{l=1}^{L}\mathbf{x}(l)\mathbf{x}^H(l), \tag{7}$$

where L denotes the number of snapshots. Obviously, $\hat{\mathbf{R}}$ is the maximum-likelihood estimator of the theoretical array covariance matrix $\mathbf{R} = E[\mathbf{x}(l)\mathbf{x}^H(l)]$, and it converges to $\mathbf{R}$ as $L \to \infty$ on the premise of stationary and ergodic assumptions [32].

B. Motivation

The motivation of the proposed coprime array adaptive beamforming algorithm can be categorized as follows.

First, coprime array offers a systematical design for sparse arrays, and has a larger array aperture than ULA with the same number of physical sensors. Considering the trade-off between the overall performance and efficiency, we prefer to perform adaptive beamforming on coprime array rather than ULA.

Second, the non-uniformity of coprime array may result in performance degradation when using the existing adaptive beamforming algorithms that designed for general array configurations. Therefore, it is important to investigate coprime feature and develop an effective beamforming algorithm tailored for the coprime array.

Third, it is quite common in mobile wireless communications that the available snapshots are limited, which leads to a large deviation between $\mathbf{R}$ and $\hat{\mathbf{R}}$. Furthermore, the signal component contained in $\hat{\mathbf{R}}$ results in signal self-nulling problem especially when the signal-to-noise ratio (SNR) is high. Therefore, enhancing the robustness of adaptive beamformer is of great importance for practical applications.

IV. Coprime Array Adaptive Beamforming

In this section, we elaborate the proposed coprime array adaptive beamforming algorithm. Based on the MVDR principle, the beamformer weight $\mathbf{w}$ in (6) is a function of the interference-plus-noise covariance matrix $\mathbf{R}_{i+n}$ and the desired signal steering vector $\mathbf{d}(\theta_s)$. With the known coprime array configuration, $\mathbf{d}(\theta_s)$ depends on the DOA of desired signal, i.e., θ_s. According to the definition of $\mathbf{R}_{i+n}$ (4), the DOAs of interferers $\{\theta_k, k = 1, 2, \ldots, K\}$ as well as their power $\{\sigma_k^2, k = 1, 2, \ldots, K\}$ and the noise power σ_n^2 are required for covariance matrix reconstruction. Therefore, we incorporate the coprime feature to perform DOA estimation and power estimation, based on which the beamformer weight is designed by reconstructing the interference-plus-noise covariance matrix and estimating the desired signal steering vector.

A. DOA Estimation Via Decomposed Coprime Sub-Arrays

Due to its sparse sensor deployment, coprime array shown in Fig. 1(b) offers a larger array aperture than ULA with the same number of sensors. Although the non-uniformity characteristic results in difficulties for analyzing and obtaining the DOA estimations by adopting existing approaches, it is encouraging that the coprime array can be regarded as a combination of a pair of sparse uniform linear sub-arrays. Therefore, we consider to process the signals received by the pair of sparse uniform linear sub-arrays as depicted in Fig. 1(a) separately. The steering vectors of the pair of sparse uniform linear sub-arrays consisting of M and N sensors are given by

$$\begin{aligned}\mathbf{d}_M(\theta) &= \left[1, e^{-\jmath\pi N\sin(\theta)}, \ldots, e^{-\jmath\pi(M-1)N\sin(\theta)}\right]^T,\\ \mathbf{d}_N(\theta) &= \left[1, e^{-\jmath\pi M\sin(\theta)}, \ldots, e^{-\jmath\pi(N-1)M\sin(\theta)}\right]^T,\end{aligned} \tag{8}$$

respectively, where $\jmath = \sqrt{-1}$. Similar to (1), the received signal vector of each sub-array can be modeled as

$$\begin{aligned}\mathbf{x}_M(l) &= \mathbf{d}_M(\theta_s)s(l) + \sum_{k=1}^{K}\mathbf{d}_M(\theta_k)i_k(l) + \mathbf{n}_M(l),\\ \mathbf{x}_N(l) &= \mathbf{d}_N(\theta_s)s(l) + \sum_{k=1}^{K}\mathbf{d}_N(\theta_k)i_k(l) + \mathbf{n}_N(l),\end{aligned} \tag{9}$$

where $i_k(l)$ denotes the k-th interference waveform, and $\mathbf{n}_M(l)$ and $\mathbf{n}_N(l)$ denote the noise vectors of the two sub-arrays, respectively. Correspondingly, their sample covariance matrices are respectively calculated as

$$\begin{aligned}\hat{\mathbf{R}}_M &= \frac{1}{L}\sum_{l=1}^{L}\mathbf{x}_M(l)\mathbf{x}_M^H(l),\\ \hat{\mathbf{R}}_N &= \frac{1}{L}\sum_{l=1}^{L}\mathbf{x}_N(l)\mathbf{x}_N^H(l).\end{aligned} \tag{10}$$

Although the sensor spacing of each sub-array is sparse, we can still use the existing DOA estimation methods designed for ULA on $\mathbf{x}_M$ and $\mathbf{x}_N$. Among them, MUltiple SIgnal Classification (MUSIC) [33] is the most famous one due to its super-resolution capability. With the sample covariance matrices of the pair of decomposed coprime sub-arrays $\hat{\mathbf{R}}_M$ and $\hat{\mathbf{R}}_N$, the MUSIC spatial spectra for each sub-array can be calculated as

$$\begin{aligned}\mathbf{p}_M(\theta) &= \frac{1}{\mathbf{d}_M^H(\theta)\mathbf{U}_M\mathbf{U}_M^H\mathbf{d}_M(\theta)},\\ \mathbf{p}_N(\theta) &= \frac{1}{\mathbf{d}_N^H(\theta)\mathbf{U}_N\mathbf{U}_N^H\mathbf{d}_N(\theta)},\end{aligned} \tag{11}$$

where $\theta \in [-90^\circ, 90^\circ]$ denotes the hypothetical direction, $\mathbf{U}_M$ and $\mathbf{U}_N$ denote the noise subspaces of $\hat{\mathbf{R}}_M$ and $\hat{\mathbf{R}}_N$, respectively. Note that although we incorporate the idea of MUSIC here as a basic step, the DOA estimations are obtained in a different manner as compared to the classical MUSIC algorithm. In general, DOA estimation can be realized by searching for the peaks in the MUSIC spatial spectrum. However, since the impinging signals are undersampled by each sub-array in a sparse way, phase ambiguity is unavoidable in $\mathbf{p}_M$ and $\mathbf{p}_N$. For the coprime array, we have the following propositions for phase ambiguity analysis.

Proposition 1: Suppose that there exists one incident source signal impinging on the coprime array. For the sub-array consisting of M sensors with an inter-element spacing of Nd, there exist N peaks in the MUSIC spatial spectrum $\mathbf{p}_M$, among which

$N-1$ peaks are the phase ambiguities. For the sub-array consisting of N sensors with an inter-element spacing of Md, there exist M peaks in the MUSIC spatial spectrum $\mathbf{p}_N$, among which $M-1$ peaks are the phase ambiguities.

Proof: See Appendix A. ■

By searching the peaks of $\mathbf{p}_M$ and $\mathbf{p}_N$, the candidate DOA sets $\Theta_M = \{\theta_{M_i} | i = 1, 2, \ldots, N(K+1)\}$ and $\Theta_N = \{\theta_{N_j} | j = 1, 2, \ldots, M(K+1)\}$ can be obtained, where the DOAs of $K+1$ incident source signals, and their phase ambiguities are included according to *Proposition 1*. In order to pick up the actual DOAs of each source from their phase ambiguities, we have the following proposition.

Proposition 2: Assuming φ to be the DOA of an incident source signal, there is one and only one same peak $\hat{\varphi}$ in both candidate DOA sets Θ_M and Θ_N, which is the estimated DOA of the incident source by using the coprime array.

Proof: See Appendix B. ■

On the basis of *Proposition 2*, we can obtain the estimated DOAs of each source by matching the common peaks in the pair of MUSIC spatial spectra $\mathbf{p}_M$ and $\mathbf{p}_N$. Note that the exactly identical DOA estimations are practically hard to find in Θ_M and Θ_N due to the background noise, we propose to find the nearest peak pair in $\mathbf{p}_M$ and $\mathbf{p}_N$ instead of searching the exactly overlapped peaks. Specifically, denoting Φ as the angular region in which the desired signal is located, we have

$$\min_{\theta_{M_i}, \theta_{N_j}} \quad \left|\theta_{M_i} - \theta_{N_j}\right|, \quad \forall\, \theta_{M_i}, \theta_{N_j} \in \Phi. \tag{12}$$

Taking the mean value of θ_{M_i} and θ_{N_j} in (12) yields the estimated DOA of desired signal by using the non-uniform coprime array, namely, $\hat{\theta}_s = (\theta_{M_i} + \theta_{N_j})/2$.

Similarly, the DOAs of interferers can be searched as

$$f_d\left(\theta_{M_i}, \theta_{N_j}\right) = \left|\theta_{M_i} - \theta_{N_j}\right| < \varepsilon, \quad \forall\, \theta_{M_i}, \theta_{N_j} \in \bar{\Phi}, \tag{13}$$

where $\bar{\Phi}$ denotes the complementary sector of Φ. That is to say, $\Phi \cup \bar{\Phi} = [-90^\circ, 90^\circ]$ and $\Phi \cap \bar{\Phi} = \emptyset$. Here, ε denotes the threshold to determine the difference of each DOA candidate pair $(\theta_{M_i}, \theta_{N_j})$ in $\bar{\Phi}$ for unique peak matching. By averaging the eligible pairs in (13), the DOAs of interferers can be estimated as $\{\hat{\theta}_1, \hat{\theta}_2, \ldots, \hat{\theta}_{\hat{K}}\}$, where $\hat{K}$ denotes the estimated number of interferers. The large array aperture of coprime array is utilized for DOA estimation through (12) and (13), and the difficulties caused by the non-uniformity of coprime array are effectively avoided through processing the received signals of each sparse uniform linear sub-array separately.

B. Power Estimation Via Joint Covariance Matrix Optimization

Up to now, we have obtained the estimated DOAs of each incident source within the angular regions of desired signal and interferers, respectively. According to (4), the power of interferers $\{\sigma_k^2, k = 1, 2, \ldots, K\}$ and the noise power σ_n^2 are also required for the reconstruction of the interference-plus-noise covariance matrix. Although it has super-resolution capability, the MUSIC spectrum is a kind of pseudo-spectrum using subspace orthogonality, which means that the spectrum response cannot reflect the actual source power. For this regard, we propose to tackle this problem by formulating a joint covariance matrix optimization problem, where the estimated source DOAs are used as *a priori* information for their power estimation.

Considering that the source signals impinge on the pair of sub-arrays simultaneously, their power components contained in $\hat{\mathbf{R}}_M$ and $\hat{\mathbf{R}}_N$ are identical although the covariance matrices are separately calculated. Therefore, the power of sources can be estimated by minimizing the difference between the sample covariance matrices $\hat{\mathbf{R}}_M$ and $\hat{\mathbf{R}}_N$ and their corresponding theoretical covariance matrices. The joint covariance matrix optimization problem is formulated Eq. (14) as shown at the bottom of this page. In (14), $\hat{\boldsymbol{\theta}} = [\hat{\theta}_s, \hat{\theta}_1, \hat{\theta}_2, \ldots, \hat{\theta}_{\hat{K}}]^T$ contains the estimated DOAs of the desired signal and interferers, $\mathbf{D}_M(\hat{\boldsymbol{\theta}}) = \left[\mathbf{d}_M(\hat{\theta}_s), \mathbf{d}_M(\hat{\theta}_1), \mathbf{d}_M(\hat{\theta}_2), \ldots, \mathbf{d}_M(\hat{\theta}_{\hat{K}})\right] \in \mathbb{C}^{M \times (\hat{K}+1)}$ and $\mathbf{D}_N(\hat{\boldsymbol{\theta}}) = \left[\mathbf{d}_N(\hat{\theta}_s), \mathbf{d}_N(\hat{\theta}_1), \mathbf{d}_N(\hat{\theta}_2), \ldots, \mathbf{d}_N(\hat{\theta}_{\hat{K}})\right] \in \mathbb{C}^{N \times (\hat{K}+1)}$ denote the steering matrices of the pair of sub-arrays. The noise power $\hat{\sigma}_n^2$ can be approximated by $(\lambda_{\min}(\hat{\mathbf{R}}_M) + \lambda_{\min}(\hat{\mathbf{R}}_N))/2$, where $\lambda_{\min}(\hat{\mathbf{R}}_M)$ and $\lambda_{\min}(\hat{\mathbf{R}}_N)$ denote the minimum eigenvalues of $\hat{\mathbf{R}}_M$ and $\hat{\mathbf{R}}_N$, respectively. The optimization variable $\boldsymbol{\Lambda} = \mathrm{diag}\left([\sigma_s^2, \sigma_1^2, \sigma_2^2, \ldots, \sigma_{\hat{K}}^2]\right)$ denotes the power of incident sources, which keeps the same in both $\hat{\mathbf{R}}_M$ and $\hat{\mathbf{R}}_N$. The positive semidefinite constraint in (14) indicates that the power of each source should be equal or greater than zero.

The optimization problem (14) is an inequality-constrained least squares problem, whose solution $\boldsymbol{\Lambda}^\star = \mathrm{diag}\left([\hat{\sigma}_s^2, \hat{\sigma}_1^2, \hat{\sigma}_2^2, \ldots, \hat{\sigma}_{\hat{K}}^2]\right)$ can be given by

$$\mathrm{diag}(\boldsymbol{\Lambda}^\star) = \left[\mathbf{B}^H \mathbf{B}\right]^{-1} \mathbf{B}^H \mathbf{r}, \tag{15}$$

where

$$\mathbf{B} = \left[\mathrm{vec}\left(\begin{bmatrix} \mathbf{d}_M(\hat{\theta}_s)\mathbf{d}_M^H(\hat{\theta}_s) & \mathbf{0} \\ \mathbf{0} & \mathbf{d}_N(\hat{\theta}_s)\mathbf{d}_N^H(\hat{\theta}_s) \end{bmatrix}\right), \ldots, \mathrm{vec}\left(\begin{bmatrix} \mathbf{d}_M(\hat{\theta}_{\hat{K}})\mathbf{d}_M^H(\hat{\theta}_{\hat{K}}) & \mathbf{0} \\ \mathbf{0} & \mathbf{d}_N(\hat{\theta}_{\hat{K}})\mathbf{d}_N^H(\hat{\theta}_{\hat{K}}) \end{bmatrix}\right)\right], \tag{16}$$

and

$$\mathbf{r} = \mathrm{vec}\left(\begin{bmatrix} \hat{\mathbf{R}}_M - \hat{\sigma}_n^2\mathbf{I} & \mathbf{0} \\ \mathbf{0} & \hat{\mathbf{R}}_N - \hat{\sigma}_n^2\mathbf{I} \end{bmatrix}\right). \tag{17}$$

$$\begin{aligned} \min_{\boldsymbol{\Lambda}} \quad & \left\| \begin{matrix} \hat{\mathbf{R}}_M - \mathbf{D}_M(\hat{\boldsymbol{\theta}})\boldsymbol{\Lambda}\mathbf{D}_M^H(\hat{\boldsymbol{\theta}}) - \hat{\sigma}_n^2\mathbf{I} & \mathbf{0} \\ \mathbf{0} & \hat{\mathbf{R}}_N - \mathbf{D}_N(\hat{\boldsymbol{\theta}})\boldsymbol{\Lambda}\mathbf{D}_N^H(\hat{\boldsymbol{\theta}}) - \hat{\sigma}_n^2\mathbf{I} \end{matrix} \right\|_F^2 \\ \text{subject to} \quad & \boldsymbol{\Lambda} \succeq \mathbf{0}, \end{aligned} \tag{14}$$

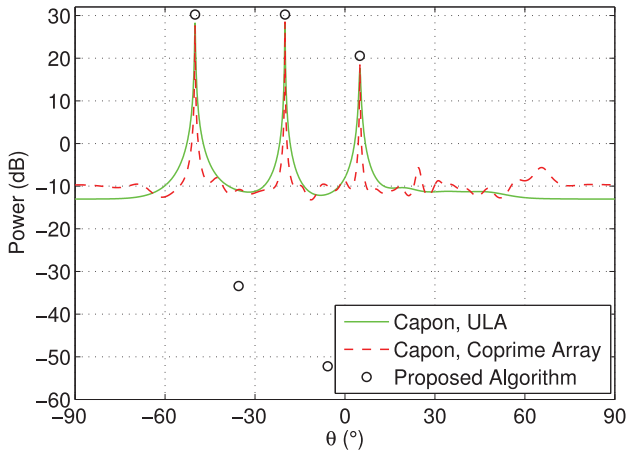

Fig. 2. Comparison of spatial spectra from one trial. There are one 20 dB desired signal from 5° and two 30 dB interferers from −50° and −20°, respectively.

To have an intuitive impression of the proposed DOA and power estimation, we illustrate the obtained sparse spatial spectrum in Fig. 2, where the pair of coprime integers is selected to be $M = 5$ and $N = 6$ for the coprime array configuration. For comparison, the Capon spatial spectra, which is utilized for covariance matrix reconstruction in [17], are also plotted with the coprime array and the ULA consisting of the same number of physical sensors. Here, the number of snapshots is set to be $L = 30$, and the threshold ε in (13) is selected to be twice the sampling interval. It is clear that the Capon spatial spectrum using coprime array enjoys a better resolution than that using ULA because of its larger array aperture. However, there also exist several extra peaks in the Capon spatial spectrum, which is mainly caused by the non-uniformity. In contrast, the proposed algorithm is able to obtain more accurate DOA and power estimation for each source. Although there are two spurious peaks as we can see, they do not affect on the following covariance matrix reconstruction because of their negligible power.

C. Proposed Beamformer Design

From (6), the MVDR beamformer depends on both interference-plus-noise covariance matrix and desired signal steering vector. Hence, we reconstruct the interference-plus-noise covariance matrix and estimate the desired signal steering vector according to the estimated DOAs of sources and their corresponding power.

With the estimated DOA $\hat{\theta}_s$, the desired signal steering vector can be calculated as

$$\mathbf{d}(\hat{\theta}_s) = \left[1, e^{-j\pi u_2 \sin(\hat{\theta}_s)}, \ldots, e^{-j\pi u_{M+N-1} \sin(\hat{\theta}_s)}\right]^T, \quad (18)$$

where $\mathbf{u} = [u_1, u_2, \ldots, u_{M+N-1}]^T$ denotes the physical sensor positions of coprime array with the reference $u_1 = 0$.

The interference-plus-noise covariance matrix can be reconstructed with the estimated DOAs of interferers and their power as

$$\hat{\mathbf{R}}_{i+n} = \sum_{k=1}^{\hat{K}} \hat{\sigma}_k^2 \mathbf{d}(\hat{\theta}_k)\mathbf{d}^H(\hat{\theta}_k) + \hat{\sigma}_n^2 \mathbf{I}, \quad (19)$$

where the interference steering vector $\mathbf{d}(\hat{\theta}_k)$ has the similar form as $\mathbf{d}(\hat{\theta}_s)$ in (18).

Following the MVDR principle, the proposed coprime array adaptive beamformer can be calculated by substituting the reconstructed interference-plus-noise covariance matrix $\hat{\mathbf{R}}_{i+n}$ in (19) and the estimated desired signal steering vector $\mathbf{d}(\hat{\theta}_s)$ in (18) into (6) as

$$\mathbf{w}_{\text{pro}} = \frac{\hat{\mathbf{R}}_{i+n}^{-1}\mathbf{d}(\hat{\theta}_s)}{\mathbf{d}^H(\hat{\theta}_s)\hat{\mathbf{R}}_{i+n}^{-1}\mathbf{d}(\hat{\theta}_s)}. \quad (20)$$

Here, the beamformer weight $\mathbf{w}_{\text{pro}} \in \mathbb{C}^{M+N-1}$ of the proposed algorithm is weighted to the coprime array received signal $\mathbf{x}(l)$, and the desired signal waveform can be estimated by calculating (2). The proposed coprime array adaptive beamforming algorithm is summarized in Algorithm 1.

Algorithm 1: Coprime Array Adaptive Beamforming.

Input: Coprime array received signals $\{\mathbf{x}(l)\}_{l=1}^{L}$;
Output: Beamformer weight $\mathbf{w}_{\text{pro}}$,
Output signal waveform $\{y(l)\}_{l=1}^{L}$;
Initialize: $\mathcal{T} = k = 1$;
Calculate MUSIC spatial spectra $\mathbf{p}_M$ and $\mathbf{p}_N$;
Obtain Θ_M and Θ_N by finding peaks in $\mathbf{p}_M$ and $\mathbf{p}_N$;
for all $\theta_{M_i} \in \Theta_M$ & $\theta_{N_j} \in \Theta_N$ **do**
  if $\theta_{M_i}, \theta_{N_j} \in \Phi$ **then**
    $\theta_{\text{diff}}^{(\mathcal{T})} = \left|\theta_{M_i} - \theta_{N_j}\right|$;
    if $\mathcal{T} > 1$ & $\theta_{\text{diff}}^{(\mathcal{T})} < \theta_{\text{diff}}^{(\mathcal{T}-1)}$ **then**
      $\hat{\theta}_s = \text{mean}\left(\theta_{M_i}, \theta_{N_j}\right)$;
    end if
    $\mathcal{T} = \mathcal{T} + 1$;
  else if $\theta_{M_i}, \theta_{N_j} \in \bar{\Phi}$ **then**
    if $\left|\theta_{M_i} - \theta_{N_j}\right| < \varepsilon$ **then**
      $\hat{\theta}_k = \text{mean}\left(\theta_{M_i}, \theta_{N_j}\right)$;
      $k = k + 1$;
    end if
  end if
end for
Solve (14) with $\hat{\theta}_s$ and $\{\hat{\theta}_k, k = 1, 2, \ldots, \hat{K}\}$;
Obtain $\hat{\sigma}_n^2$ by averaging $\lambda_{\min}(\hat{\mathbf{R}}_M)$ and $\lambda_{\min}(\hat{\mathbf{R}}_N)$;
Estimate $\mathbf{d}(\hat{\theta}_s)$ by (18) with $\hat{\theta}_s$;
Reconstruct $\hat{\mathbf{R}}_{i+n}$ by (19) with $\hat{\theta}_k$, $\hat{\sigma}_k^2$, and $\hat{\sigma}_n^2$;
Calculate $\mathbf{w}_{\text{pro}}$ (20) by substituting $\mathbf{d}(\hat{\theta}_s)$ and $\hat{\mathbf{R}}_{i+n}$;
Output signal waveform $y(l) = \mathbf{w}_{\text{pro}}^H \mathbf{x}(l)$.

V. Theoretical Analyses

In this section, we present the theoretical analyses for the proposed coprime array adaptive beamforming algorithm in

terms of robustness to threshold selection and computational efficiency.

A. Threshold Selection for Interferer Identification

In (13), we introduce a threshold ε for the DOA estimation of interferers, which plays a key role in determining the eligible pair of candidate DOA pairs $\left(\theta_{M_i}, \theta_{N_j}\right)$ within $\bar{\Phi}$. Since the number of interferers is not available in practice, we usually select a relaxed threshold for interferer identification instead of adopting an ideal one. Here, we will discuss the impact of threshold selection on the output SINR performance.

It is defined in (3) that the output SINR is a function of the beamformer weight $\mathbf{w}$, and the solution to the MVDR principle (6) yields optimal output SINR. That is to say, both the reconstructed interference-plus-noise covariance matrix $\hat{\mathbf{R}}_{i+n}$ and the estimated signal steering vector $\mathbf{d}(\hat{\theta}_s)$ affect the output SINR performance. Considering the fact that the threshold ε only determines the estimated DOAs of interferers, we focus on the performance deviation caused by $\hat{\mathbf{R}}_{i+n}$ in this subsection.

To achieve an optimal output SINR, one of the preconditions should be the reconstructed interference-plus-noise covariance matrix trends to its theoretical version, i.e., $\hat{\mathbf{R}}_{i+n} \to \mathbf{R}_{i+n}$. Apart from the actual $K+1$ sources $\hat{\boldsymbol{\theta}}_{\mathcal{K}} = [\hat{\theta}_s, \hat{\theta}_1, \hat{\theta}_2, \ldots, \hat{\theta}_K]$, the additional $\hat{K} - K$ DOA estimations $\hat{\boldsymbol{\theta}}_{\mathcal{A}} = [\hat{\theta}_{K+1}, \hat{\theta}_{K+2}, \ldots, \hat{\theta}_{\hat{K}}]$ caused by the relaxed threshold ε contribute the deviation in the interference-plus-noise covariance matrix reconstruction process (19) as

$$\Delta\mathbf{R}_{\mathrm{Th}} = \sum_{k=K+1}^{\hat{K}} \hat{\sigma}_k^2 \mathbf{d}(\hat{\theta}_k)\mathbf{d}^H(\hat{\theta}_k). \tag{21}$$

Considering that the power of each estimated DOA in $\hat{\boldsymbol{\theta}}$ is obtained from the joint covariance matrix optimization problem (14), to analyse the deviation $\Delta\mathbf{R}_{\mathrm{Th}}$, we reformulate its objective function as

$$\begin{aligned} e_{\mathcal{U}} = &\left\|\hat{\mathbf{R}}_M - \mathbf{D}_M(\hat{\boldsymbol{\theta}})\boldsymbol{\Lambda}\mathbf{D}_M^H(\hat{\boldsymbol{\theta}}) - \hat{\sigma}_n^2\mathbf{I}\right\|_F^2 \\ &+ \left\|\hat{\mathbf{R}}_N - \mathbf{D}_N(\hat{\boldsymbol{\theta}})\boldsymbol{\Lambda}\mathbf{D}_N^H(\hat{\boldsymbol{\theta}}) - \hat{\sigma}_n^2\mathbf{I}\right\|_F^2. \end{aligned} \tag{22}$$

Denoting the diagonal matrices $\boldsymbol{\Lambda}_{\mathcal{K}}^{\star}$ and $\boldsymbol{\Lambda}_{\mathcal{A}}^{\star}$ respectively contain the estimated power of $\hat{\boldsymbol{\theta}}_{\mathcal{K}}$ and $\hat{\boldsymbol{\theta}}_{\mathcal{A}}$ in (15), we have

$$\begin{aligned} e_{\mathcal{U}} \le &\left\|\hat{\mathbf{R}}_M - \mathbf{D}_M(\hat{\boldsymbol{\theta}}_{\mathcal{K}})\boldsymbol{\Lambda}_{\mathcal{K}}^{\star}\mathbf{D}_M^H(\hat{\boldsymbol{\theta}}_{\mathcal{K}}) - \hat{\sigma}_n^2\mathbf{I}\right\|_F^2 \\ &+ \left\|\mathbf{D}_M(\hat{\boldsymbol{\theta}}_{\mathcal{A}})\boldsymbol{\Lambda}_{\mathcal{A}}^{\star}\mathbf{D}_M^H(\hat{\boldsymbol{\theta}}_{\mathcal{A}})\right\|_F^2 \\ &+ \left\|\hat{\mathbf{R}}_N - \mathbf{D}_N(\hat{\boldsymbol{\theta}}_{\mathcal{K}})\boldsymbol{\Lambda}_{\mathcal{K}}^{\star}\mathbf{D}_N^H(\hat{\boldsymbol{\theta}}_{\mathcal{K}}) - \hat{\sigma}_n^2\mathbf{I}\right\|_F^2 \\ &+ \left\|\mathbf{D}_N(\hat{\boldsymbol{\theta}}_{\mathcal{A}})\boldsymbol{\Lambda}_{\mathcal{A}}^{\star}\mathbf{D}_N^H(\hat{\boldsymbol{\theta}}_{\mathcal{A}})\right\|_F^2. \end{aligned} \tag{23}$$

Considering the fact that $\hat{\mathbf{R}}_M$ and $\hat{\mathbf{R}}_N$ are the maximum likelihood estimator of the sub-array pair theoretical covariance matrices $\mathbf{R}_M = E\left[\mathbf{x}_M(l)\mathbf{x}_M^H(l)\right]$ and $\mathbf{R}_N = E\left[\mathbf{x}_N(l)\mathbf{x}_N^H(l)\right]$, the corresponding differences can be minimized as long as the DOA and power of the $K+1$ actual sources are accurately estimated, namely,

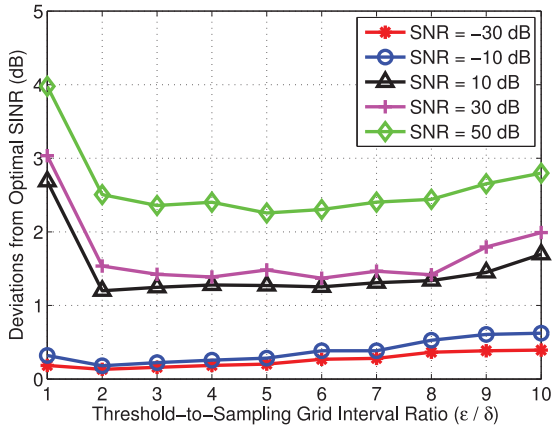

Fig. 3. Deviations from optimal SINR performance of the proposed algorithm versus threshold-to-sampling interval ratio with $L = 30$.

$$\begin{aligned} &\lim_{\substack{\hat{\theta}_k \to \theta_k, \hat{\sigma}_k^2 \to \sigma_k^2 \\ k=s,1,2,\ldots,K}} \left\|\hat{\mathbf{R}}_M - \mathbf{D}_M(\hat{\boldsymbol{\theta}}_{\mathcal{K}})\boldsymbol{\Lambda}_{\mathcal{K}}^{\star}\mathbf{D}_M^H(\hat{\boldsymbol{\theta}}_{\mathcal{K}}) - \hat{\sigma}_n^2\mathbf{I}\right\|_F^2 = \zeta_M, \\ &\lim_{\substack{\hat{\theta}_k \to \theta_k, \hat{\sigma}_k^2 \to \sigma_k^2 \\ k=s,1,2,\ldots,K}} \left\|\hat{\mathbf{R}}_N - \mathbf{D}_N(\hat{\boldsymbol{\theta}}_{\mathcal{K}})\boldsymbol{\Lambda}_{\mathcal{K}}^{\star}\mathbf{D}_N^H(\hat{\boldsymbol{\theta}}_{\mathcal{K}}) - \hat{\sigma}_n^2\mathbf{I}\right\|_F^2 = \zeta_N. \end{aligned} \tag{24}$$

Here, ζ_M and ζ_N are the constants close to zero, which denote the inherent deviation of the approximated sample covariance matrices. Therefore, on the premise of accurate DOA and power estimation for the $K+1$ sources, the problem of minimizing $e_{\mathcal{U}}$ in (22) can be simplified to minimize the following function

$$\begin{aligned} &\mathcal{G}(\boldsymbol{\Lambda}_{\mathcal{A}}^{\star}, \hat{\boldsymbol{\theta}}_{\mathcal{A}}) \\ &= \left\|\mathbf{D}_M(\hat{\boldsymbol{\theta}}_{\mathcal{A}})\boldsymbol{\Lambda}_{\mathcal{A}}^{\star}\mathbf{D}_M^H(\hat{\boldsymbol{\theta}}_{\mathcal{A}})\right\|_F^2 + \left\|\mathbf{D}_N(\hat{\boldsymbol{\theta}}_{\mathcal{A}})\boldsymbol{\Lambda}_{\mathcal{A}}^{\star}\mathbf{D}_N^H(\hat{\boldsymbol{\theta}}_{\mathcal{A}})\right\|_F^2. \end{aligned} \tag{25}$$

Since the DOA estimations in $\hat{\boldsymbol{\theta}}_{\mathcal{A}}$ contribute an additional deviation component $\mathcal{G}(\boldsymbol{\Lambda}_{\mathcal{A}}^{\star}, \hat{\boldsymbol{\theta}}_{\mathcal{A}})$ in $e_{\mathcal{U}}$, an optimal solution for (22) yields $\mathcal{G}(\boldsymbol{\Lambda}_{\mathcal{A}}^{\star}, \hat{\boldsymbol{\theta}}_{\mathcal{A}}) \to 0$ without loss of generality. While $\mathcal{G}(\boldsymbol{\Lambda}_{\mathcal{A}}^{\star}, \hat{\boldsymbol{\theta}}_{\mathcal{A}})$ is a function of $\boldsymbol{\Lambda}_{\mathcal{A}}^{\star}$ and $\hat{\boldsymbol{\theta}}_{\mathcal{A}}$, and $\hat{\boldsymbol{\theta}}_{\mathcal{A}}$ is the ready-made DOA estimations as *a priori*, it is clear that $\boldsymbol{\Lambda}_{\mathcal{A}}^{\star} \to \mathbf{0}$ when $\mathcal{G}(\boldsymbol{\Lambda}_{\mathcal{A}}^{\star}, \hat{\boldsymbol{\theta}}_{\mathcal{A}})$ converges to zero. Taking the constraint $\boldsymbol{\Lambda} \succeq \mathbf{0}$ of (14) into consideration, the power estimation for each estimated DOAs in $\hat{\boldsymbol{\theta}}_{\mathcal{A}}$ converges to zero, which implies that the deviation component $\Delta\mathbf{R}_{\mathrm{Th}} \to \mathbf{0}$. Therefore, the additional DOA estimations only occupy a negligible proportion in the reconstructed interference-plus-noise covariance matrix $\hat{\mathbf{R}}_{i+n}$, which means the relaxed threshold will not cause obvious output SINR performance degradation.

The output performance deviations from optimal SINR of the proposed algorithm versus the ratio of threshold ε to sampling interval δ is plotted in Fig. 3, where the number of snapshots is $L = 30$, and the other parameters are the same as in Example 1 of Section VI. According to (13), the threshold parameter setting is related to the sampling interval of the hypothetical direction δ. Here, we select the threshold varying from 0.1° to 1°, which is

equal to one to ten-fold of the sampling interval δ. It is demonstrated that the SINR deviation of the proposed algorithm is relatively stable when the threshold ε is chosen to be twice the sampling interval δ or larger under different input SNR cases. The reason can be interpreted that the additional $\hat{K} - K$ DOA estimations resulted from the relaxed threshold ε can be *identified* through power estimation process, and the corresponding estimated power is negligible, which can be verified in Fig. 2.

Unlike the *DOA estimation* problem, the number of interferers K is not a necessary information for our *coprime array adaptive beamforming* algorithm, and the relaxed threshold will not cause severe output performance degradation due to the associated power estimation. Therefore, the threshold selection in the proposed algorithm is flexible, where the robustness is demonstrated in terms of threshold parameter setting.

B. Complexity Analysis

The computational complexity of the proposed coprime array adaptive beamforming algorithm is $\mathcal{O}((M^2 + N^2)G)$, where $G >> M + N$ denotes the number of hypothetical directions in $\mathbf{p}_M$ and $\mathbf{p}_N$. In contrast, the covariance matrix reconstruction-based beamforming algorithm [17], which directly operates on the coprime array received signals, has a computational complexity of $\mathcal{O}((M + N)^2 G)$. Both the sample matrix inversion (SMI) beamforming algorithm [34] and the diagonal loading SMI (DLSMI) beamforming algorithm [35] are $\mathcal{O}((M + N)^3)$, which is dominated by the covariance matrix inversion. Due to the necessity eigenvalue decomposition, the eigenspace-based beamforming algorithm [36] has a computational complexity of $\mathcal{O}((M + N)^3)$. The optimization problem in the worst-case performance optimization-based beamforming algorithm [37] also generates an $\mathcal{O}((M + N)^3)$ computational complexity.

Therefore, the proposed coprime array adaptive beamforming algorithm enjoys a higher computational efficiency than the covariance matrix reconstruction-based beamforming algorithm [17]. The reason lies in that the proposed algorithm operates the signals received by the pair of sub-arrays separately, where the MUSIC spatial spectra $\mathbf{p}_M$ and $\mathbf{p}_N$ are calculated with less sensors than the original coprime array. Although the computational complexity of the proposed algorithm is slightly larger than the classical beamforming algorithms [34]–[37], it can be further decreased to $\mathcal{O}(M^3 + N^3)$ by incorporating search-free techniques, such as root-MUSIC [38], to the DOA estimation process (11), so that the number of hypothetical directions G can be significantly decreased. By contrast, the search-free techniques cannot be incorporated to the covariance matrix reconstruction-based beamforming algorithm [17], since it requires to integrate over the entire hypothetical directions for reconstruction. Moreover, the efficiency of the proposed algorithm can also be further improved by adopting advanced spectrum searching schemes [26], [39] in DOA estimation process.

In order to demonstrate the efficiency of adaptive beamformer exploiting coprime array, here we would also compare the computational complexity with the existing beamforming algorithms using ULA. As shown in Fig. 1, the coprime array has an array aperture of $\max\big((M-1)Nd, (N-1)Md\big)$ with only $M + N - 1$ physical sensors. If a ULA with the physical sensors spaced half-wavelength apart is deployed for achieving the same array aperture, $\max(MN - M + 1, MN - N + 1)$ physical sensors are required, which means the computational complexity of covariance matrix reconstruction-based beamforming algorithm [17] increases to $\mathcal{O}((MN)^2 G)$. Also, the computational complexity of SMI, DLSMI, eigenspace-based as well as the worst-case-based beamforming algorithm becomes to $\mathcal{O}((MN)^3)$. Therefore, performing adaptive beamforming on coprime array is capable to significantly decrease the computational complexity as compared to ULA.

Apart from the computational complexity, the hardware complexity is also an important issue in practical applications. With a coprime array, fewer physical sensors are required as well as the associated radio frequency chains, where the overall cost for the practical system can be significantly reduced. Therefore, the efficiency of the proposed coprime array adaptive beamforming algorithm is demonstrated in both computational complexity and hardware complexity.

Based on the above analyses, the proposed coprime array adaptive beamforming algorithm enjoys the following advantages. First, the coprime feature is effectively utilized to perform parameter estimation, while the performance degradation caused by its non-uniformity is avoided. Second, the number of sources is not a necessary requirement for DOA estimation in the proposed algorithm, since the power estimation is capable to avoid the deviation caused by the additional DOA estimations. Third, the proposed coprime array adaptive beamforming algorithm is more efficient than the existing algorithms using ULA.

VI. Simulation

In this section, we evaluate the performance of the proposed coprime array adaptive beamforming algorithm. In particular, we consider several typical propagation scenarios in practical mobile wireless communication applications, and compare the performance of the proposed algorithm against existing adaptive beamforming algorithms.

In our simulations, a coprime array consisting of 10 omnidirectional sensors is deployed with the coprime integers $M = 5$ and $N = 6$. Accordingly, the pair of decomposed sparse uniform linear sub-arrays is located at $[0, 6, 12, 18, 24]d$ and $[0, 5, 10, 15, 20, 25]d$, respectively. The desired signal is assumed to be from the direction $\theta_s = 5^\circ$, while two interferers are assumed to have the directions $\theta_1 = -50^\circ$ and $\theta_2 = -20^\circ$. The additive noise is modeled as a zero-mean white Gaussian random process. The interference-to-noise ratio (INR) at each sensor is chosen to be 30 dB. For output SINR performance comparison, the input SNR is fixed at 20 dB when we vary the number of snapshots, whereas the number of snapshots is fixed at $L = 30$ when we vary the input SNR. For each scenario, 1,000 Monte-Carlo trials are performed.

The proposed algorithm is compared to the SMI beamforming algorithm [34], the DLSMI beamforming algorithm [35], the eigenspace-based beamforming algorithm [36], the worst-case-based beamforming algorithm [37], and the covariance matrix reconstruction-based beamforming algorithm [17]. It is

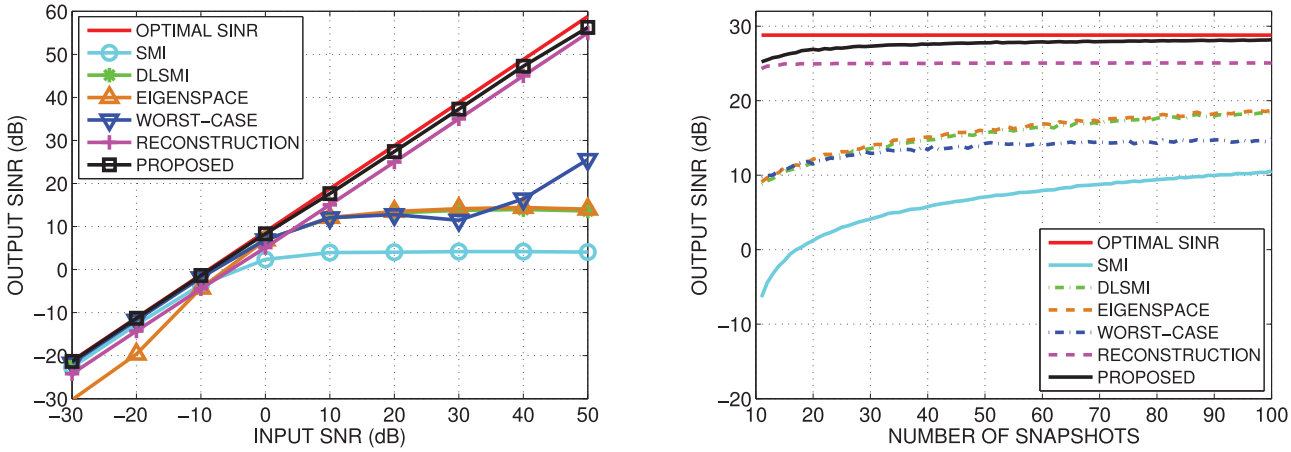

(a) (b)

Fig. 4. First example: exactly known desired signal steering vector. (a) Output SINR versus the input SNR; (b) output SINR versus the number of snapshots.

worth noting that, unlike the proposed algorithm, the other adaptive beamforming algorithms use the received signal of the coprime array to design their beamformer weight vectors as they did conventionally. For the proposed algorithm and the one in [17], we assume the angular region of the desired signal to be $\Phi = [\theta_s - 5^\circ, \theta_s + 5^\circ]$. The angular region of the interferers is the complementary sector of Φ, namely, $\bar{\Phi} = [-90^\circ, \theta_s - 5^\circ) \cup (\theta_s + 5^\circ, 90^\circ]$. The hypothetical direction θ for the spatial spectra $\mathbf{p}_M$ and $\mathbf{p}_N$ is uniformly sampled on $[-90^\circ, 90^\circ]$ with sampling interval $\delta = 0.1^\circ$. The threshold ε in (13) is chosen to be twice the sampling interval δ, i.e., $\varepsilon = 0.2^\circ$. The diagonal loading factor is selected to be $10\sigma_n^2$ for the DLSMI beamformer [35], and the upper bound of the norm of steering vector distortion for the worst-case-based beamformer [37] is $\epsilon = 0.15 \times (M + N - 1)$. The optimal SINR is also plotted in all figures for reference.

A. Example 1: Exactly Known Desired Signal Steering Vector

In the first example, we consider a scenario that the desired signal steering vector is exactly known. The output SINR of each algorithm versus input SNR and the number of snapshots is depicted in Fig. 4(a) and (b), respectively.

We can observe from Fig. 4(a) that the output SINRs of the SMI, DLSMI, and eigenspace-based beamformers become relatively flat rather than keep increasing with the increase of the input SNR. The reason lies in that the sample covariance matrix $\hat{\mathbf{R}}$ is utilized in these adaptive beamformers, where the sample covariance matrix contaminated by the desired signal component fails to approach the theoretical interference-plus-noise covariance matrix especially at high SNRs. Although the bounded norm of the steering vector mismatch is considered in the worst-case-based beamforming algorithm, there still exists performance degradation due to the utilization of $\hat{\mathbf{R}}$ in the beamformer design. By contrast, the reconstruction-based algorithms outperform the others as expected, and their output SINRs are close to the optimal SINR since the desired signal is excluded from the reconstructed covariance matrix. Benefited from more accurate power estimation than the Capon spatial spectrum, the proposed coprime array adaptive beamforming algorithm outperforms the reconstruction-based beamforming algorithm in [17] almost in the entire considered SNR range. When the performance is compared in terms of the number of snapshots, we can also find that the output SINR of the proposed algorithm is closer to the optimal SINR than the reconstruction-based one [17] according to Fig. 4(b).

B. Example 2: Fixed Signal Look Direction Mismatch

In the second example, we simulate the scenario due to fixed signal look direction mismatch. The actual desired signal and the presumed signal are assumed to have the directions of 8° and 5°, respectively. That is to say, there exists a 3° fixed signal look direction mismatch. The output SINR curves against the input SNR and the number of snapshots are shown in Fig. 5(a) and (b), respectively.

It can be seen from Fig. 5(a) that the SMI, DLSMI, eigenspace-based, and worst-case-based beamformers suffer from obvious performance degradation, which is caused by the steering vector mismatch due to direction mismatch. While the signal steering vector in the proposed algorithm is calculated from the estimated DOA, it is demonstrated in Fig. 5(a) that the output SINR of the proposed beamformer is almost overlapped with the optimal SINR when input SNR is larger than 0 dB. Therefore, the proposed algorithm is robust to fixed signal look direction mismatch. Besides, there exists about 10 dB output SINR performance advantage for the proposed algorithm than the covariance matrix reconstruction-based beamforming algorithm [17] when the input SNR is larger than 0 dB. Except the steering vector mismatch, the integration over the Capon spatial spectrum also results in the output performance degradation for the covariance matrix reconstruction-based beamforming algorithm [17]. Similar comparison results can also be found in Fig. 5(b), where the output SINR curve of the proposed algorithm closely overlaps with the optimal SINR even for the limited snapshot case. It is common that the number of available snapshots for adaptive beamformer weight design is relatively limited in mobile wireless communications. Hence, the stable

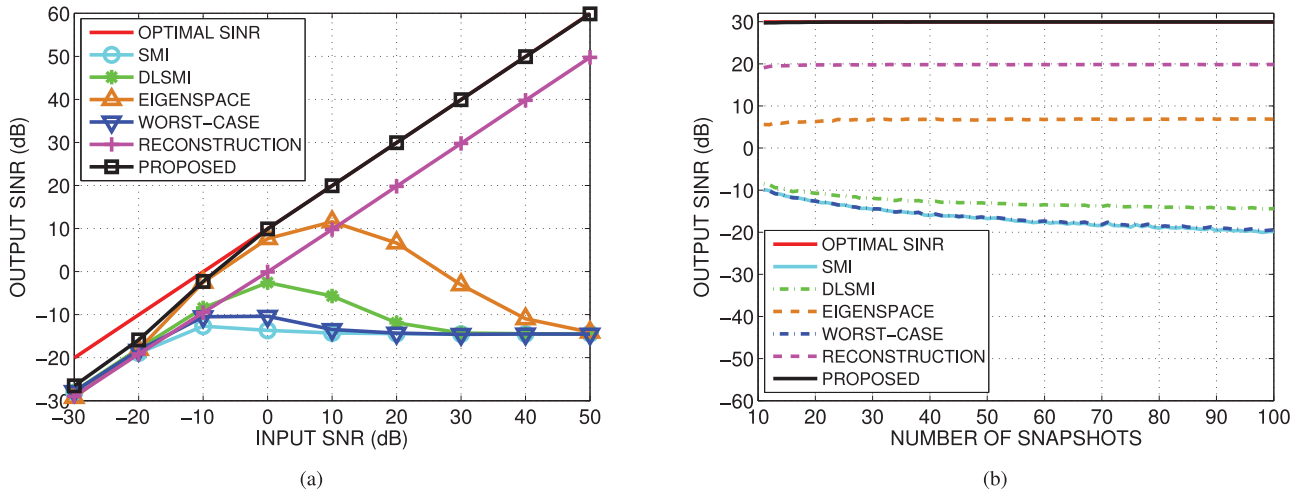

Fig. 5. Second example: fixed signal look direction mismatch. (a) Output SINR versus the input SNR; (b) output SINR versus the number of snapshots.

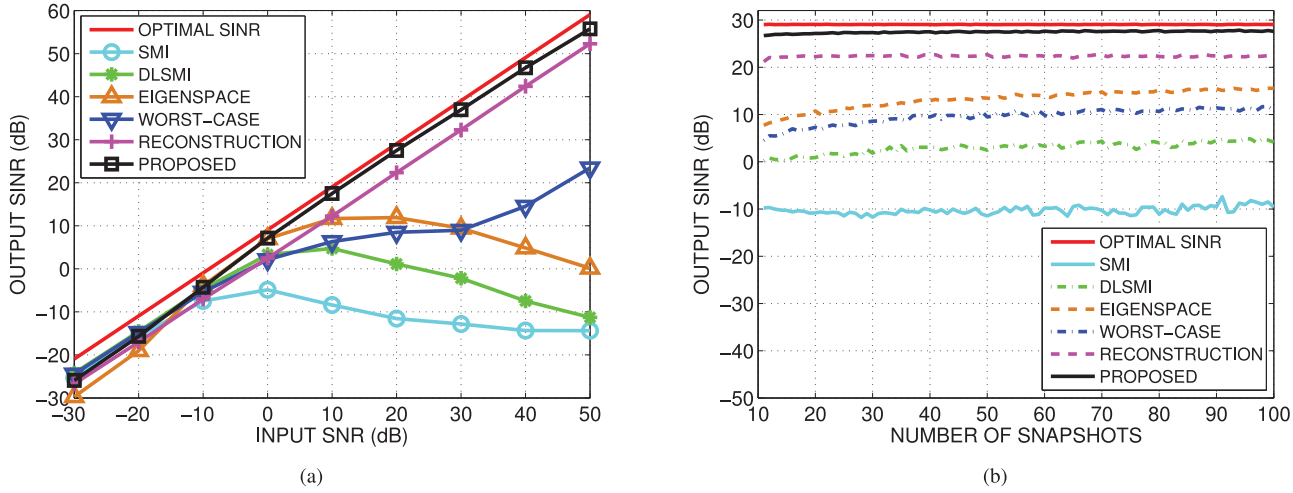

Fig. 6. Third example: random signal look direction mismatch. (a) Output SINR versus the input SNR; (b) output SINR versus the number of snapshots.

output performance under different numbers of snapshots indicates that the proposed algorithm is a reliable technique for high-mobility applications.

C. Example 3: Random Signal Look Direction Mismatch

In the third example, the random signal look direction mismatch is considered. More specifically, we assume that both the desired signal and the interferers have a random signal look direction mismatch subject to a uniform distribution in $[-4^\circ, 4^\circ]$. That is to say, the direction of desired signal is randomly chosen within $[1^\circ, 9^\circ]$, and the directions of two interferers are randomly chosen within $[-54^\circ, -46^\circ]$ and $[-24^\circ, -16^\circ]$, respectively. The source directions change from trial to trial but keep fixed from snapshot to snapshot. The comparison results are illustrated in Fig. 6(a) and (b).

Similar to the performance comparisons shown in Fig. 5(a), both the approximated sample covariance matrix and the presumed steering vector cause the performance loss for the SMI, DLSMI, and the eigenspace-based beamformers especially when SNR is high. Although the worst-case-based beamformer combats the random signal look direction mismatch in some extent, its output performance is still inferior to the reconstruction-based algorithms. By contrast, the output SINR of the proposed algorithm outperforms the others in terms of both input SNR and the number of snapshots. The reason for the superiority can be mainly categorized into two aspects. First, both the interference-plus-noise covariance matrix and the desired signal steering vector of the proposed algorithm are obtained according to the estimated DOA and power of each incident source, which estimation accuracy will directly affect the output performance. Second, benefiting from the coprime feature of the coprime array as well as its large array aperture, both the DOA and power can be effectively estimated. Therefore, the proposed algorithm is robust to random signal look direction mismatch, which is a realistic advantage for the practical applications, such as time-varying wireless communication systems.

D. Example 4: Mismatch Caused by Wavefront Distortion

In the fourth example, we assume that the spatial signature of the desired signal is affected by wave propagation effects in an

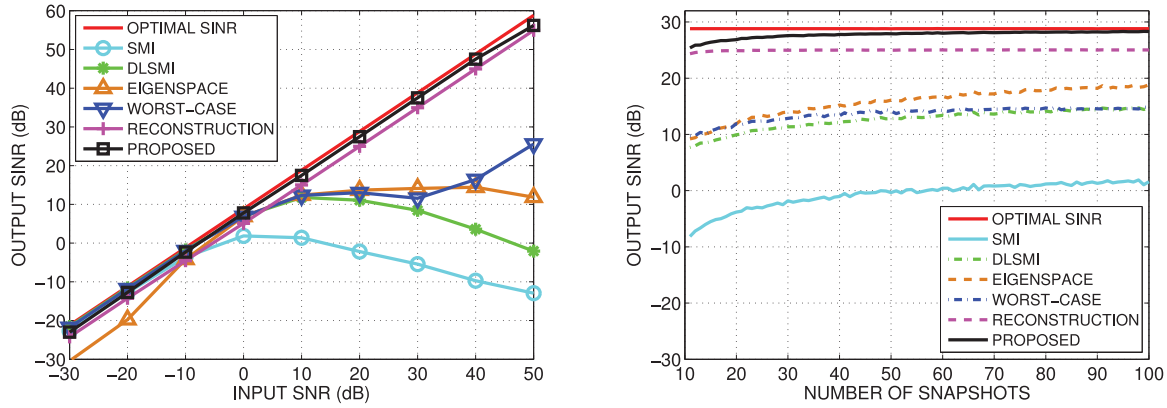

Fig. 7. Fourth example: wavefront distortion. (a) Output SINR versus the input SNR; (b) output SINR versus the number of snapshots.

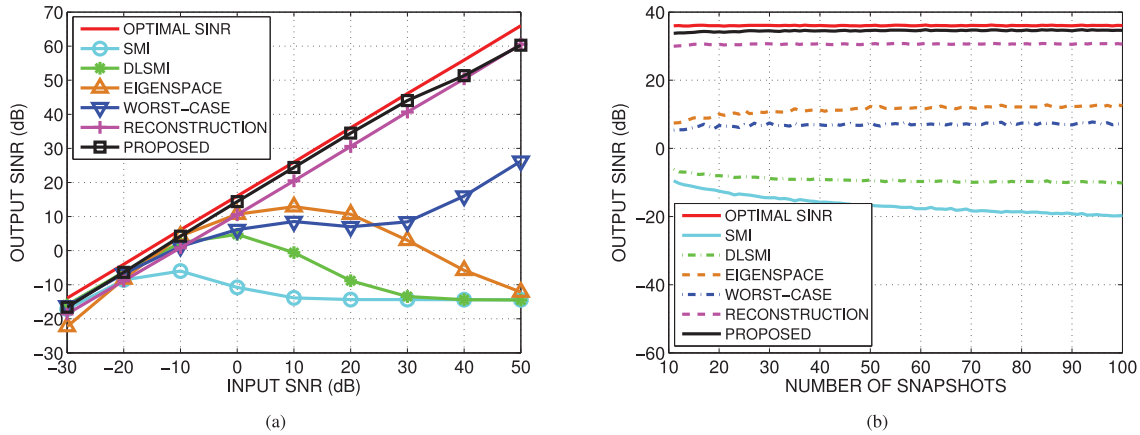

Fig. 8. Fifth example: coherent local scattering. (a) Output SINR versus the input SNR; (b) output SINR versus the number of snapshots.

inhomogeneous medium, where independent-increment phase distortions of the desired signal wavefront are accumulated and the array steering vector is distorted. The phase increment in each trial is drawn from an independent Gaussian random generator $\mathcal{N}(0, 0.04)$.

According to the simulation results depicted in Fig. 7(a) and (b), it is clear that the proposed algorithm performs much better than the other adaptive beamforming algorithms, which indicates that both DOA and power estimation are effective for the model mismatch case caused by wavefront distortion. In contrast, the model mismatch deviates the output SINR of the other algorithms for comparison as we learn from Fig. 7(a). Hence, the robustness of the coprime array adaptive beamformer can be guaranteed by reconstructing the interference-plus-noise covariance matrix and estimating the desired signal steering vector jointly.

E. Example 5: Mismatch Caused by Coherent Local Scattering

In the last example, we consider the mismatch caused by coherent local scattering, as commonly encountered in mobile communications in the form of multipath propagation. Assuming that the spatial signature of the desired signal is distorted by local scattering effects, the actual array steering vector is formed by five signal paths, which consist of one direct path and four coherently scattered paths as

$$\tilde{\mathbf{d}} = \bar{\mathbf{d}} + \sum_{p=1}^{4} e^{\jmath\phi_p}\,\mathbf{d}(\psi_p), \tag{26}$$

where $\bar{\mathbf{d}}$ denotes the presumed steering vector with the incident plane wave signal from the direction $\theta_s = 5^\circ$, and $\mathbf{d}(\psi_p)$ denotes the p-th coherently scattered path which can be viewed as a plane wave signal from ψ_p. The path directions $\{\psi_p, p = 1, 2, 3, 4\}$ are independently and identically distributed in a Gaussian distribution with mean θ_s and standard deviation 2°; the path phases $\{\phi_p, p = 1, 2, 3, 4\}$ are independently and uniformly distributed in $[0, 2\pi]$. Both parameters ψ_p and ϕ_p change from trial to trial but remain fixed from snapshot to snapshot.

The output SINR of each algorithm is displayed in Fig. 8(a) and (b). Unlike the aforementioned scenarios, there is an extra 6 dB output SINR increment for the optimal beamformer because of the existing multipath. Nevertheless, the proposed algorithm still outperforms the others in the whole range we considered. Because the extra multipaths disturb both the sample covariance matrix and the steering vector, there are performance losses at high SNRs. The comparisons demonstrate that the proposed algorithm is robust to the model mismatch caused by coherent local scattering.

VII. Conclusion

In this paper, we proposed a novel coprime array adaptive beamforming algorithm. Coprime array provides a larger array aperture than ULA with the same number of sensors; hence, it improves the resolution with a reasonable computational complexity. DOA estimation and power estimation are sequentially performed by processing the received signals of the pair of sparse uniform linear sub-arrays decomposed from the coprime array, where the properties of coprime integers are exploited. The estimated DOAs and power are utilized to reconstruct the interference-plus-noise covariance matrix and estimate the desired signal steering vector. Finally, the proposed coprime array adaptive beamformer weight vector is designed based on MVDR principle. Theoretical analyses are provided to verify the robustness and efficiency of the proposed coprime array adaptive beamforming algorithm. Extensive simulation results demonstrate that the proposed algorithm is robust to several typical model mismatches in mobile wireless communications and achieves a better output performance than the other adaptive beamforming algorithms.

Appendix A
Proof of Proposition 1

Proof: We first consider the sparse uniform linear sub-array consisting of M sensors spaced Nd apart. Denoting φ_k^a as the ambiguous angle of the k-th incident source φ_k, according to the definition of the sub-array steering vector (8), the phase ambiguity condition can be formulated as [26]

$$\sin(\varphi_k) - \sin(\varphi_k^a) = \frac{2V_M}{N}, \tag{27}$$

where V_M is a non-zero integer variable.

On the other hand, for any φ_k and φ_k^a within $[-90^\circ, 90^\circ]$, we have

$$|\sin(\varphi_k) - \sin(\varphi_k^a)| < 2. \tag{28}$$

Substituting (27) into (28), the condition that there exists phase ambiguity yields

$$\left|\frac{2V_M}{N}\right| < 2, \tag{29}$$

where $2(N-1)$ solutions can be found for V_M, namely, $V_M = -(N-1), -(N-2), \ldots, -1, 1, \ldots, N-2, N-1$. Since φ_k and φ_k^a are interconvertible in (28), $N-1$ solutions are available for V_M in (29). Except the actual estimated DOA of the incident source φ_k, the angles corresponding to the $N-1$ solutions of V_M in (27) are the phase ambiguities. Therefore, there exist N peaks in the MUSIC spatial spectrum $\mathbf{p}_M$, among which $N-1$ peaks are the phase ambiguities.

Similarly, for the sparse uniform linear sub-array consisting of N sensors spaced Md apart, we can readily formulate the corresponding phase ambiguity condition as

$$\left|\frac{2V_N}{M}\right| < 2, \tag{30}$$

where $V_N = -(M-1), -(M-2), \ldots, -1, 1, \ldots, M-2, M-1$. Therefore, there exist M peaks in the MUSIC spatial spectrum $\mathbf{p}_N$, among which $M-1$ peaks are the phase ambiguities. ■

Appendix B
Proof of Proposition 2

Proof: We present the proof of this proposition from the perspective of existence and uniqueness, respectively.

Existence: If $\hat{\varphi}$ is the estimated DOA of the incident source φ by using the coprime array, it must present a peak in the MUSIC spatial spectrum of the coprime array shown in Fig. 1(b). Obviously, both the MUSIC spatial spectra $\mathbf{p}_M$ and $\mathbf{p}_N$ contain a peak at the same position regardless of the different ambiguous peaks.

Uniqueness: Assume that there exists another DOA estimation $\hat{\varphi}'$ at the same position of both MUSIC spatial spectra $\mathbf{p}_M$ and $\mathbf{p}_N$ except $\hat{\varphi}$, according to (27), we have

$$\sin(\hat{\varphi}') - \sin(\hat{\varphi}) = \frac{2V_M}{N}, \tag{31}$$

$$\sin(\hat{\varphi}') - \sin(\hat{\varphi}) = \frac{2V_N}{M}, \tag{32}$$

which correspond to the MUSIC spatial spectra $\mathbf{p}_M$ and $\mathbf{p}_N$, respectively. Combining (31) and (32) yields

$$\frac{2V_M}{N} = \frac{2V_N}{M}, \tag{33}$$

i.e.,

$$V_M M = V_N N. \tag{34}$$

Since the greatest common factor of the coprime integers M and N is one, we cannot find any eligible pair $\{V_M, V_N\}$ to fulfill (34). Hence, $\hat{\varphi}$ is the unique DOA estimation of the incident source φ by using the coprime array. ■

References

[1] C. Zhou, Y. Gu, W.-Z. Song, Y. Xie, and Z. Shi, "Robust adaptive beamforming based on DOA support using decomposed coprime subarrays," in *Proc. IEEE ICASSP*, Shanghai, China, Mar. 2016, pp. 2986–2990.

[2] H. L. Van Trees, *Detection, Estimation, and Modulation Theory, Part IV: Optimum Array Processing*. New York, NY: Wiley, 2002.

[3] R. Pec, B. W. Ku, K. S. Kim, and Y. S. Cho, "Receive beamforming techniques for an LTE-based mobile relay station with a uniform linear array," *IEEE Trans. Veh. Technol.*, vol. 64, no. 7, pp. 3299–3304, Jul. 2015.

[4] Q. Shi, L. Liu, W. Xu, and R. Zhang, "Joint transmit beamforming and receive power splitting for MISO SWIPT systems," *IEEE Trans. Wireless Commun.*, vol. 13, no. 6, pp. 3269–3280, Jun. 2014.

[5] B. Liao, K. M. Tsui, and S. C. Chan, "Robust beamforming with magnitude response constraints using iterative second-order cone programming," *IEEE Trans. Antennas Propag.*, vol. 59, no. 9, pp. 3477–3482, Sep. 2011.

[6] B. Hu, C. Hua, C. Chen, X. Ma, and X. Guan, "MUBFP: Multi-user beamforming and partitioning for sum capacity maximization in MIMO systems," *IEEE Trans. Veh. Technol.*, vol. 66, no. 1, pp. 233–245, Jan. 2017.

[7] X. Lin, M. Tao, Y. Xu, and R. Wang, "Outage probability and finite-SNR diversity–multiplexing tradeoff for two-way relay fading channels," *IEEE Trans. Veh. Technol.*, vol. 62, no. 7, pp. 3123–3136, Sep. 2013.

[8] J. Mo, M. Tao, Y. Liu, and R. Wang, "Secure beamforming for MIMO two-way communications with an untrusted relay," *IEEE Trans. Signal Process.*, vol. 62, no. 9, pp. 2185–2199, May 2014.

[9] J. Li and P. Stocia, Eds. *Robust Adaptive Beamforming*. New York, NY: Wiley, 2005.

[10] P. P. Vaidyanathan and P. Pal, "Sparse sensing with co-prime samplers and arrays," *IEEE Trans. Signal Process.*, vol. 59, no. 2, pp. 573–586, Feb. 2011.
[11] Z. Shi, C. Zhou, Y. Gu, N. A. Goodman, and F. Qu, "Source estimation using coprime array: A sparse reconstruction perspective," *IEEE Sensors J.*, vol. 17, no. 3, pp. 755–765, Feb. 2017.
[12] K. Han and A. Nehorai, "Wideband Gaussian source processing using a linear nested array," *IEEE Signal Process. Lett.*, vol. 20, no. 11, pp. 1110–1113, Nov. 2013.
[13] C. Zhou, Z. Shi, Y. Gu, and N. A. Goodman, "DOA estimation by covariance matrix sparse reconstruction of coprime array," in *Proc. IEEE Int. Conf. Acoust., Speech, Signal Process. (ICASSP)*, Brisbane, Australia, Apr. 2015, pp. 2369–2373.
[14] Y. D. Zhang, M. G. Amin, and B. Himed, "Sparsity-based DOA estimation using co-prime arrays," in *Proc. IEEE Int. Conf. Acoust., Speech, Signal Process. (ICASSP)*, Vancouver, Canada, May 2013, pp. 3967–3971.
[15] P. Pal and P. P. Vaidyanathan, "Coprime sampling and the MUSIC algorithm," in *Proc. IEEE Digit. Signal Process. Workshop/IEEE Signal Process. Educ. Workshop*, Sedona, AZ, Jan. 2011, pp. 289–294.
[16] Y. Gu, C. Zhou, N. A. Goodman, W.-Z. Song, and Z. Shi, "Coprime array adaptive beamforming based on compressive sensing virtual array signal," in *Proc. IEEE Int. Conf. Acoust., Speech, Signal Process. (ICASSP)*, Shanghai, China, Mar. 2016, pp. 2981–2985.
[17] Y. Gu and A. Leshem, "Robust adaptive beamforming based on interference covariance matrix reconstruction and steering vector estimation," *IEEE Trans. Signal Process.*, vol. 60, no. 7, pp. 3881–3885, Jul. 2012.
[18] Y. Gu, N. A. Goodman, S. Hong, and Y. Li, "Robust adaptive beamforming based on interference covariance matrix sparse reconstruction," *Signal Process.*, vol. 96, pp. 375–381, Mar. 2014.
[19] Y. Gu and A. Leshem, "Robust adaptive beamforming based on jointly estimating covariance matrix and steering vector," in *Proc. IEEE Int. Conf. Acoust., Speech, Signal Process. (ICASSP)*, Prague, Czech Republic, May 2011, pp. 2640–2643.
[20] L. Zhao, W.-Z. Song, X. Ye, and Y. Gu, "Asynchronous broadcast-based decentralized learning in sensor networks," *Int. J. Parallel, Emergent Distrib. Syst.*, pp. 1–19, Mar. 2017.
[21] Y. Liu, J. R. Buck, and R. Bautista, "Spatial power spectral estimation using coprime sensor array with the min processor," *J. Acoust. Soc. Amer.*, vol. 139, no. 4, pp. 2109–2110, Apr. 2016.
[22] B. Wang, Y. D. Zhang, and W. Wang, "Robust group compressive sensing for DOA estimation with partially distorted observations," *EURASIP J. Adv. Signal Process.*, vol. 2016, no. 2016:128, pp. 1–10, Dec. 2016.
[23] Y. Zhou, W. Xu, H. Zhao, and N. R. Chapman, "Improving statistical robustness of matched-field source localization via general-rank covariance matrix matching," *IEEE J. Ocean. Eng.*, vol. 41, no. 2, pp. 395–407, Apr. 2016.
[24] G. Shou, L. Xia, F. Liu, M. Jiang, and S. Crozier, "On epicardial potential reconstruction using regularization schemes with the l1-norm data term," *Phys. Med. Biol.*, vol. 56, no. 1, pp. 57–72, Jan. 2011.
[25] Z. Weng and P. M. Djurić, "A search-free DOA estimation algorithm for coprime arrays," *Digit. Signal Process.*, vol. 24, pp. 27–33, Jan. 2014.
[26] C. Zhou, Z. Shi, Y. Gu, and X. Shen, "DECOM: DOA estimation with combined MUSIC for coprime array," in *Proc. Int. Conf. Wireless Commun. Signal Process. (WCSP)*, Hangzhou, China, Oct. 2013, pp. 1–5.
[27] C. Zhou, Z. Shi, and Y. Gu, "Coprime array adaptive beamforming with enhanced degrees-of-freedom capability," in *Proc. IEEE Radar Conf.*, Seattle, WA, May 2017, pp. 1357–1361.
[28] S. Qin, Y. D. Zhang, M. G. Amin, and A. M. Zoubir, "Generalized coprime sampling of Toeplitz matrices for spectrum estimation," *IEEE Trans. Signal Process.*, vol. 65, no. 1, pp. 81–94, Jan. 2017.
[29] X. Wu, W.-P. Zhu, and J. Yan, "Direction-of-arrival estimation based on Toeplitz covariance matrix reconstruction," in *Proc. IEEE Int. Conf. Acoust., Speech, Signal Process. (ICASSP)*, Shanghai, China, Mar. 2016, pp. 3071–3075.
[30] X. Fan, C. Zhou, Y. Gu, and Z. Shi, "Toeplitz matrix reconstruction of interpolated coprime virtual array for DOA estimation," in *Proc. IEEE Veh. Technol. Conf. (VTC2017-Spring)*, Sydney, Australia, Jun. 2017, pp. 1–5.
[31] J. Capon, "High-resolution frequency-wavenumber spectrum analysis," *Proc. IEEE*, vol. 57, no. 8, pp. 1408–1418, Aug. 1969.
[32] N. R. Goodman, "Statistical analysis based on a certain multivariate complex Gaussian distribution (An introduction)," *Ann. Math. Statist.*, vol. 34, no. 1, pp. 152–177, Mar. 1963.
[33] R. O. Schmidt, "Multiple emitter location and signal parameter estimation," *IEEE Trans. Antennas Propag.*, vol. 34, no. 3, pp. 276–280, Mar. 1986.
[34] I. S. Reed, J. D. Mallett, and L. E. Brennan, "Rapid convergence rate in adaptive arrays," *IEEE Trans. Aerosp. Electron. Syst.*, vol. 10, no. 6, pp. 853–863, Nov. 1974.
[35] H. Cox, R. M. Zeskind, and M. M. Owen, "Robust adaptive beamforming," *IEEE Trans. Acoust., Speech, Signal Process.*, vol. 35, no. 10, pp. 1365–1376, Oct. 1987.
[36] D. D. Feldman and L. J. Griffiths, "A projection approach for robust adaptive beamforming," *IEEE Trans. Signal Process.*, vol. 42, no. 4, pp. 867–876, Apr. 1994.
[37] S. A. Vorobyov, A. B. Gershman, and Z.-Q. Luo, "Robust adaptive beamforming using worst-case performance optimization: A solution to the signal mismatch problem," *IEEE Trans. Signal Process.*, vol. 51, no. 2, pp. 313–324, Feb. 2003.
[38] B. D. Rao and K. V. S. Hari, "Performance analysis of root-music," *IEEE Trans. Acoust., Speech, Signal Process.*, vol. 37, no. 12, pp. 1939–1949, Dec. 1989.
[39] D. Malioutov, M. Çetin, and A. S. Willsky, "A sparse signal reconstruction perspective for source localization with sensor arrays," *IEEE Trans. Signal Process.*, vol. 53, no. 8, pp. 3010–3022, Aug. 2005.

Chengwei Zhou (S'15) received the B.E. degree in communication engineering from Zhejiang Sci-Tech University, Hangzhou, China, in 2013. He is currently working toward the Ph.D. degree in the College of Information Science and Electronic Engineering, Zhejiang University, Hangzhou, China. His current research interests include the areas of array signal processing, compressive sensing, and wireless communications.

Yujie Gu (M'10–SM'16) received the B.E. degree in mechanical engineering from Harbin Institute of Technology, Harbin, China, in 2001, the M.S. degree in control engineering from Sichuan University, Chengdu, China, in 2004, and the Ph.D. degree in electrical engineering from Zhejiang University, Hangzhou, China, in 2008. After graduation, he was an R&D Engineer at CETC 51, Shanghai, China. From 2009 to 2010, he was in the Department of Electrical and Computer Engineering, Concordia University, Montréal, QC, Canada. From 2010 to 2011, he was with the School of Engineering, Bar-Ilan University, Ramat-Gan, Israel. In 2012, he worked as an Associate Professor at the Shanghai Advanced Research Institute, Chinese Academy of Sciences, Shanghai, China. After that, he was with the School of Electrical and Computer Engineering and the Advanced Radar Research Center, the University of Oklahoma, Norman, OK, USA, and the Department of Computer Science, Georgia State University, Atlanta, GA, USA, and he is currently with the Department of Electrical and Computer Engineering, Temple University, Philadelphia, PA, USA. His research interests include statistical and array signal processing.

Dr. Gu received the ReSMiQ Postdoctoral Scholarship from Microsystems Strategic Alliance of Québec, Montréal, QC, Canada, in 2009. He is an Associate Member of the Sensor Array and Multichannel (SAM) Technical Committee of the IEEE Signal Processing Society. He serves on the Editorial Boards of *Signal Processing*, *Electronics Letters*, *IET Signal Processing*, *Circuits, Systems and Signal Processing* and the *Journal on Advances in Signal Processing*. He has been a Member of the Technical Program Committee of several international conferences, including IEEE ICASSP, SAM, and CoSeRa.

Shibo He (M'13) received the Ph.D. degree in control science and engineering from Zhejiang University, Hangzhou, China, in 2012.

From November 2010 to November 2011, he was a Visiting Scholar in the University of Waterloo, Waterloo, ON, Canada. He was an Associate Research Scientist from March 2014 to May 2014, and a postdoctoral scholar from May 2012 to February 2014, with Arizona State University, Tempe, AZ, USA. He is currently a Professor at Zhejiang University. His research interests include wireless sensor networks, crowdsensing, and big data analysis. He is on the editorial board of the IEEE TRANSACTIONS ON VEHICULAR TECHNOLOGY, Springer *Peer-to-Peer Networking and Application*, *KSII Transactions on Internet and Information Systems*, and is a Guest Editor of Elsevier *Computer Communications* and Hindawi *International Journal of Distributed Sensor Networks*. He served as publicity chair for IEEE SECON 2016, Registration and Fiance chair for ACM MobiHoc 2015, TPC Co-Chair for IEEE ScalCom 2014, TPC Vice Co-Chair for ANT 2013-2014, Track Co-Chair for the Pervasive Algorithms, Protocols, and Networks of EUSPN 2013, Web Co-Chair for IEEE MASS 2013, and Publicity Co-Chair of IEEE WiSARN 2010. He coauthored two papers that won the best paper award of IEEE PIRMC 2012 and IEEE WCNC 2017. In 2015, he received the IEEE Asia-Pacific outstanding researcher award.

Zhiguo Shi (M'09–SM'15) received the B.S. and Ph.D. degrees in electronic engineering from Zhejiang University, Hangzhou, China, in 2001 and 2006, respectively. Since 2006, he has been a faculty member in the College of Information Science and Electronic Engineering, Zhejiang University, where he is currently a Full Professor. From September 2011 to November 2013, he was visiting the Broadband Communications Research Group at the University of Waterloo. He is currently an Editor for the IEEE NETWORK, and *IET Communications*.